Appl Phys A (2011) 103: 689–692
DOI 10.1007/s00339-011-6335-y

Applied Physics A
Materials Science & Processing

Tunable THz metamaterials based on an array of paraelectric $SrTiO_3$ rods

R. Yahiaoui · H. Němec · P. Kužel · F. Kadlec · C. Kadlec · P. Mounaix

Received: 8 January 2010 / Accepted: 3 December 2010 / Published online: 16 February 2011

Abstract This work presents theoretical and experimental investigations of a tunable metamaterial which exhibits negative permeability in the THz frequency range. The tunability is obtained by temperature changes, and the sample consists of an array of high-permittivity $SrTiO_3$ (STO) rods micromachined by a femtosecond laser. Structures exhibiting a negative permeability on multiple frequency bands are also investigated and a proper choice of the dimensions of the pattern allows us to achieve a substantial broadening of the frequency band with negative μ.

1 Introduction

During the last decade, the concept of metamaterials has been conceived and a variety of metamaterial structures was extensively investigated. Most of the works are inspired by the structures proposed initially by Pendry [1] and deal with metamaterials based on a dielectric substrate with subwavelength metallic patterns. Another approach, focusing on the Mie resonances of dielectric particles [2, 3], leads to a different class of metamaterials. In this work, we propose the description and the numerical study of a dielectric tunable metamaterial where the tunability is achieved by a temperature variation of the permittivity. We also present an extension of this structure, which simultaneously exhibits several magnetic resonances in sub mm range. Finally, we study the impact of the geometry on the frequency broadening of the band with $\mu < 0$. Our investigated metamaterials may offer a possibility to bridge the gap between the microwave and optical frequencies.

R. Yahiaoui · P. Mounaix (✉)
Laboratoire Ondes et Matière d'Aquitaine, UMR CNRS 5798,
Université Bordeaux I, 351 Cours de la Libération,
33405 Talence cedex, France
e-mail: p.mounaix@loma.u-bordeaux1.fr

H. Němec · P. Kužel (✉) · F. Kadlec · C. Kadlec
Institute of Physics, Academy of Sciences, Na Slovance 2,
182 21 Prague 8, Czech Republic
e-mail: kuzelp@fzu.cz

2 Response of the metamaterial

Our sample, as shown in Fig. 1(a) consists of a high-permittivity dielectric material ($SrTiO_3$) with a thickness $t = 52$ µm which was micromachined by a femtosecond laser to obtain a series of bars (width $w = 42.5$ µm) separated by air gaps $g = 32.5$ µm. Figure 1(b) shows a scanning electron microscopy image of the structure. The sample is illuminated by a plane wave at normal incidence, with the magnetic field parallel to the x axis ($H \parallel x$ axis) and the electric field parallel to the y axis ($E \parallel y$ axis). The resulting propagation direction is along the z axis ($\boldsymbol{k} \parallel z$ axis). Figure 2(a) and (b) shows the theoretical and experimental magnitude and phase of the transmittance which are obtained using the transfer matrix method and time-domain terahertz spectroscopy, respectively.

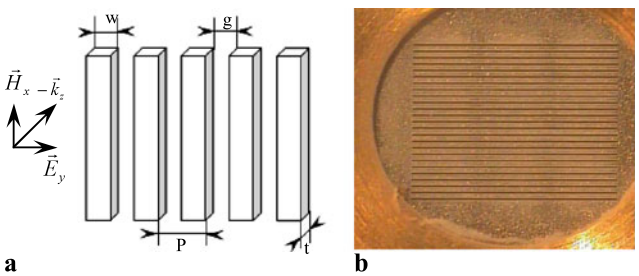

Fig. 1 (**a**) Schematic view of the structure, (**b**) scanning electron microscopy image of our metamaterial

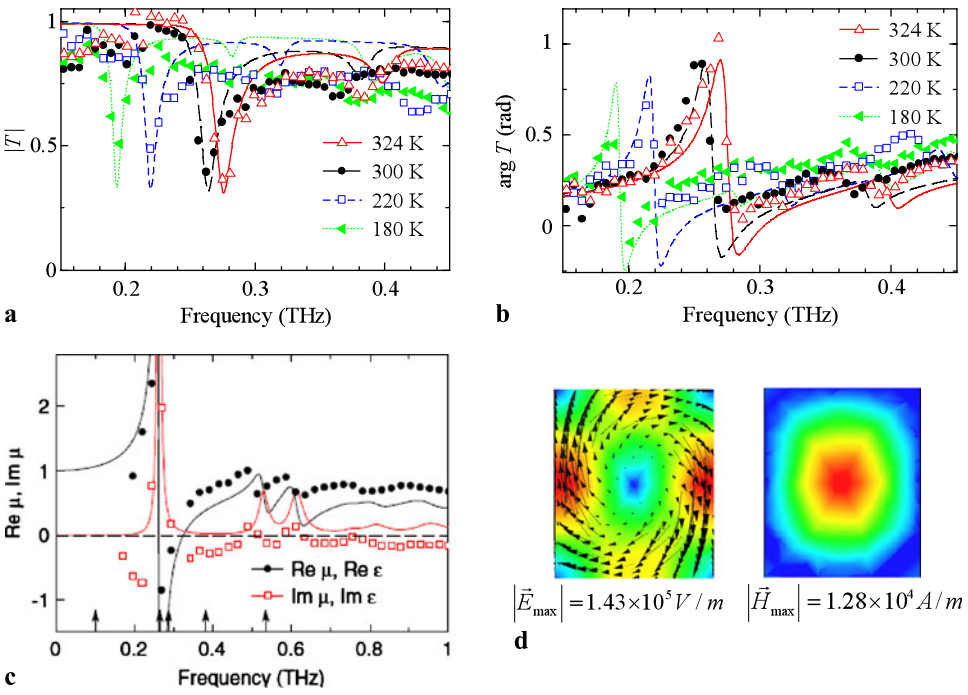

Fig. 2 (**a**) Theoretical and experimental transmission spectrum, (**b**) theoretical and experimental transmission phase, (**c**) theoretical and experimental magnetic response at room temperature, (**d**) electric and magnetic field distribution at the lowest-frequency Mie resonance

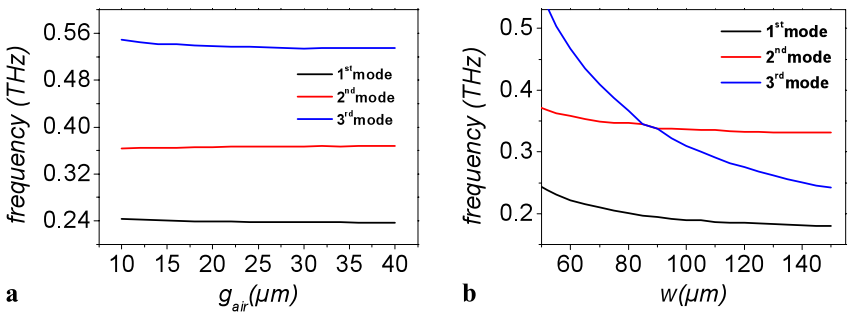

Fig. 3 (**a**) Resonant frequencies as a function of the air gap width g. (**b**) Resonant frequencies as a function of w

The response has been tuned from 0.2 THz to 0.28 THz by changing the temperature from 180 K to 324 K. Under the given polarisation of magnetic and electric field, magnetic resonances are observed which induce negative values of the effective permeability. Figure 2(c) shows a good agreement between the experimental and the calculated magnetic response. The effective permittivity and permeability are retrieved by applying an extraction procedure described in [4]. For a better understanding of the physical processes involved within the structure, we use an electromagnetic software simulator HFSS based on the finite-element method to calculate the electric and magnetic field distribution within the rods (Fig. 2(d)). The calculation was done for the first resonant mode ∼0.28 THz at 324 K. The wave front of an incident plane wave is subject to a strong distortion close to the metamaterial in order to satisfy simultaneously the continuity and discontinuity conditions of tangential and normal electric-field components at the STO-air interfaces, respectively [4, 5]. The electric field, which develops inside an STO bar, is predominantly tangential close to the surface of the bar. This leads to the creation of displacive eddy currents within the bar cross section, which enhance the magnetic field inside STO along the bar. The resonant behaviour is then expected at specific frequencies.

In order to asses the impact of the air gap width g and of the lateral dimension w on the position of the resonant modes of the metamaterial, we, respectively, varied g within 10–40 μm and w within 50–150 μm, while the other dimensions of the rods were fixed in such cases. Figure 3(a) and (b) shows the result of this parametric study, which confirms that g has no influence on the position of the magnetic modes; however, the resonance frequency presents a hyperbolic decrease as a function of the lateral dimension w.

3 A multiple frequency bands metamaterial

A series of works concerning metamaterials which operate at multiple frequency bands have been undertaken at microwave frequencies [6], in the terahertz regime [7, 8] and

even at optical frequencies [9]. In this section, in order to extend the negative permeability region of our metamaterial to several frequency bands, we designed a structure with a set of rods with various widths. Figure 4(a) shows the unit cell of the metamaterial designed, which consists of rods with three different widths a, b, and c, respectively, separated by the same the air gap width g, the thickness t of the rods remains constant; we consider an infinite array of such rods in x- and y-directions (Fig. 4(a)). According to Fig. 4(b) where $\mu = \mu_1 + i\mu_2$, we note that the effective permeability μ is a superposition of the responses of each individual rod, the highlighted zones correspond to the negative permeability regions. We have also calculated the distributions of the magnetic field for the resonance frequencies 0.24 THz, 0.334 THz and 0.458 THz, respectively (not shown here), which clearly show that the mutual cross couplings are negligible [5].

4 Broadband negative permeability metamaterial

A broadband planar and non-planar negative refractive index metamaterial based on traditional split ring resonators and wires are reported by Wongkasem et al. [10]. In this section, we propose to design an STO based metamaterial which exhibits a much-broader negative permeability band. The investigated metamaterial consists of a single type of rods with a width w (varied from 50 μm to 200 μm in our study), while $g = 30$ μm and $t = 20$ μm are kept constant. A broadening of the range with negative μ is achieved with a high aspect ratio ($w \gg t$). The polarisation of the electromagnetic wave is the same as those described in previous sections. The amplitude transmittance and the real part of effective permeability for each value of w are depicted in Fig. 5(b) and (b).

We note that the position of the first Mie resonance does not shift significantly upon the change of w. In fact, it is mainly imposed by the thickness t of the metamaterial for $w > 100$ μm. By contrast, upon increasing w, the distance between the first and higher order resonances is reduced, and the resonances overlap for $w \gg t$ [see Fig. 5(a)]. This leads to a broadening of the region of negative μ [Fig. 5(b)]. For example, the retrieved effective μ for $w = 50$ μm is negative within 480–600 GHz, but for higher rod widths this range is much broader; namely for $w = 200$ μm it spans over 250 GHz, corresponding to nearly 50% of the central frequency value. Figure 6(a) and (b) shows the real and imaginary part of the effective permeability, respectively, for $w = 200$ μm and for the values of the loss tangent of STO ($\tan\delta$) varying from 0.1% to 5%. According to Fig. 6(a), we note that the frequency band of negative permeability widens, only if the dielectric losses reach a sufficiently high level ($\tan\delta > 1\%$). Upon the increase of $\tan\delta$, the amplitude of real part of μ decreases more and more, and a similar behaviour is observed for the imaginary part of μ (see Fig. 6(b)). Further analysis reveals a compromise between a high negative μ limited by the value of $\tan\delta$ and a large bandwidth where μ is negative. Finally, we propose optimal geometric dimensions of the structure of $w = 200$ μm, $g = 30$ μm, $t = 20$ μm, which leads to a negative permeability within a frequency band from 430 to 680 GHz.

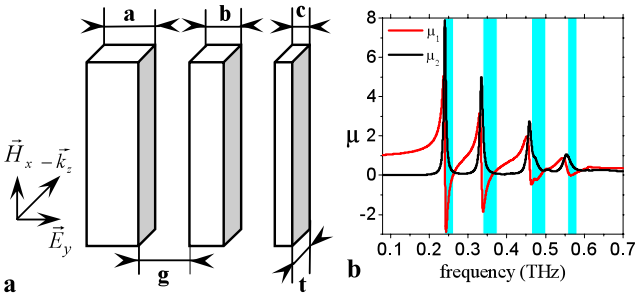

Fig. 4 (**a**) Schematic view of the investigated metamaterial with the geometrical dimension: $a = 50$ μm, $b = 30$ μm, $c = 20$ μm, $g = 20$ μm; (**b**) Calculated spectra of effective μ for the corresponding structure; (**c**) Sections of a unit cell of the metamaterial with the spatial distribution of the resonant magnetic field; (**d**) Effective permeability for different values of air gap

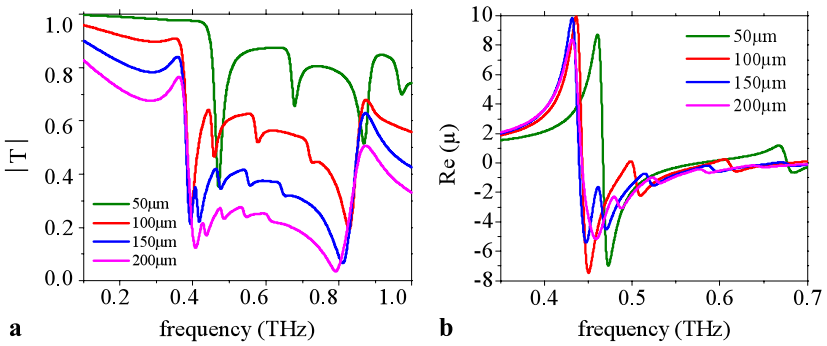

Fig. 5 (**a**) Calculated amplitude transmittance for several widths w of STO rods ($g = 30$ μm, $t = 20$ μm, $\tan\delta = 2.5\%$), (**b**) the corresponding effective permeability

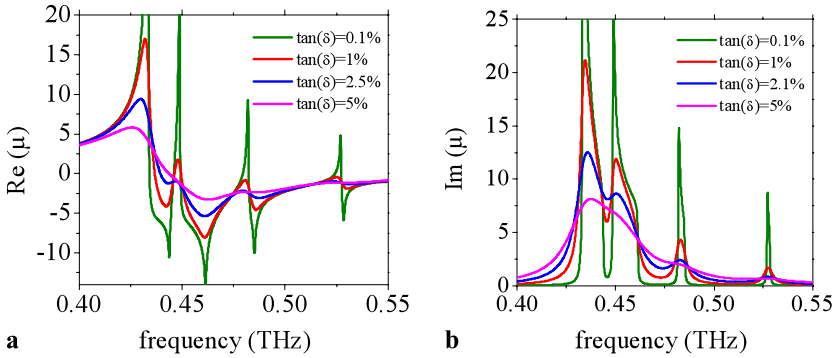

Fig. 6 (**a**) Real part of μ, (**b**) imaginary part of μ for $w = 200$ μm and $\tan\delta$ from 0.1% to 5%

5 Conclusion

The dielectric metamaterial presented made of $SrTiO_3$ rods in this work exhibits a negative effective permeability which was tuned by temperature. A smart choice of the lateral dimensions of the rods of the metamaterial can lead to a negative permeability over a wide frequency range.

Acknowledgements This work was initiated at the University of Bordeaux 1 under the project "GIS métamatériaux". Financial support from the Ministry of Education of the Czech Republic (project LC-512) and of the Grant Agency of ASCR (project A100100907) is acknowledged.

References

1. B. Pendry, A.J. Holden, D.J. Robbins, W.J. Stewart, Magnetism from conductors and enhanced nonlinear phenomena. IEEE Trans. Microw. Theory Tech. **47**, 2075 (1999)
2. K.C. Huang, M.L. Povinelli, J.D. Joannopoulos, Negative effective permeability in polaritonic photonic crystals. Appl. Phys. Lett. **85**, 543 (2004)
3. Q. Zhao, L. Kang, B. Du, H. Zhao, Q. Xie, X. Huang, B. Li, J. Zhou, L. Li, Experimental demonstration of isotropic negative permeability in a three-dimensional dielectric composite. Phys. Rev. Lett. **101**, 027402 (2008)
4. H. Němec, P. Kužel, F. Kadlec, C. Kadlec, R. Yahiaoui, P. Mounaix, Tunable terahertz metamaterials with negative permeability. Phys. Rev. B **79**, 241108(R) (2009)
5. R. Yahiaoui, H. Němec, P. Kužel, F. Kadlec, C. Kadlec, P. Mounaix, Broadband dielectric terahertz metamaterials with negative permeability. Opt. Lett. **34**, 3541 (2009)
6. H. Chen, L. Ran, J. Huangfu, X. Zhang, K. Chen, T.M. Grzegorczyk, J.A. Kong, Metamaterial exhibiting left-handed properties over multiple frequency bands. J. Appl. Phys. **96**, 5338 (2004)
7. Y. Yuan, C. Bingham, T. Tyler, S. Palit, T.H. Hand, W.J. Padilla, N.M. Jokerst, S.A. Cummer, A dual-resonant terahertz metamaterial based on single-particle electric-field-coupled resonators. Appl. Phys. Lett. **93**, 191110 (2008)
8. Y. Yuan, C. Bingham, T. Tyler, S. Palit, T.H. Hand, W.J. Padilla, D.R. Smith, N.M. Jokerst, S.A. Cummer, Dual-band planar electric metamaterial in the terahertz regime. Opt. Express **16**, 9746 (2008)
9. N. Shen, M. Kafesaki, T. Koschny, L. Zhang, E.N. Economou, C.M. Soukoulis, Broadband blue shift tunable metamaterials and dual-band switches. Phys. Rev. B **79**, 161102(R) (2009)
10. N. Wongkasem, A. Akyurtlu, J. Li, A. Tibolt, Z. Kang, W.D. Goodhue, Novel broadband terahertz negative refractive index metamaterials: analysis and experiment. Prog. Electromagn. Res. **64**, 205 (2006)